Chapter

Modeling and Simulation in Microwave-Photonics Applications

Mikhail E. Belkin, Tatiana Bakhvalova, Vladislav Golovin, Yuriy Tyschuk and Alexander S. Sigov

Abstract

In this chapter, with the goal to recover an optimal mean for computer-aided modeling and simulating a newer class of microwave-photonics-based radio electronic apparatuses, a number of comparative simulation experiments for the basic microwave band electronic devices and systems using well-known software tools referred to photonic design automation or upgraded electronic design automation platforms are carried out. As a result, it is shown that exploiting the software of upgraded electronic design automation platform provides significantly better accuracy of calculations for the devices and systems of this class.

Keywords: computer-aided design, microwave photonics, radio electronic apparatus

1. Introduction

Nowadays, microwave photonics (MWP) is a relatively mature scientific and technological direction arising among radio electronic R&D society at the second half of the twentieth century in result of combining the achievements of microwave electronics and photonics techniques [1]. Initially, MWP was an area of interest for a military platform [2, 3] such as radar and electronic warfare means, but recent years, it became an object of study and development for emerging areas in the telecommunication industry [4] such as fifth-generation (5G) cellular networks. For today, MWP technology might be considered as a perspective direction of modern radio electronics for signal generation, transmission, and processing in various radio frequency (RF) circuits and systems of microwave (MW) band. Implementation of this concept will enhance the key technical and economical features and such important characteristics as electromagnetic and environmental compatibilities, immunity to external interferences.

Following this tendency, we have contributed some works referred to computer-aided design of MWP components and MWP-based devices [5–18] using two well-known software tools such as VPI Photonics Design Suite (VPI-PDS) [19] and Applied Wave Research Design Environment (AWRDE) [20]. Elaborating the direction, in this chapter, we review shortly the distinctive features of MWP technique, preselecting an optimal software to computer-aided design (CAD), a hybrid device combining microwave electronics and photonics components. After that, we highlight our last modeling and simulation results on design and optimization

of advanced microwave and millimeter-wave band RF electronic facilities based on MWP technique, mainly for an access network of 5G mobile communication systems. In particular, Section 2 reviews the nature, features, and space of the MWP approach to develop advanced radio electronics apparatuses (REAs). In addition, Section 3 presents a short comparative analysis of modern computer platforms with the goal of selecting a feasible mean to design MWP-based REA. The examples for comparative computer-aided simulations of key optical and optoelectronics elements, such as laser, optical modulator, photodetector, and optical fiber, as well as based on them specific MWP devices and apparatuses for microwave-signal processing in optical range such as a delay circuit, oscillator, frequency converter, and fiber-wireless fronthaul of 5G mobile communication system, are demonstrated in Section 4. All schemes are simulated in VPI-PDS and AWRDE CAD tools. Finally, Section 5 concludes the chapter.

2. The distinctive features of MWP technique

Microwave photonics is a rather fresh interdisciplinary scientific-technical and scientific-technological direction of radio electronics and photonics, which provides an increase in the efficiency of the formation and processing of analog and digital radio signals due to their transfer to the optical range. The use of MWP in promising radio facilities for various purposes has the potential, first, from the point of view of increasing operating frequencies up to tens of terahertz, ensuring their multirange, multifunctionality, reconfigurability, and increasing speed and throughput in accordance with modern requirements. Another purpose of MWP is to improve the performance characteristics of existing REAs such as instantaneous bandwidth, electromagnetic compatibility, power consumption, reliability, resistance to natural and intentional interference, footprint, and environmental friendliness.

Generally, MWP devices are the examples of an intimate integration of photonics, microwave electronics, and planar antenna technologies for producing a complicated functional module in a multichannel analog environment. In particular, MWP technology opens the way to superwide bandwidth transmitting characteristics at lower size, weight, and power as compared with traditional electronic information and communication systems [2, 3]. For example, it is expected that this direction will find wide application in the RF equipment for accessing networks of incoming mobile communication systems with distribution in the millimeter-wave range [4, 17]. **Figure 1** demonstrates a typical MWP arrangement, where for direct and inverse transferring of MW and optical signals, two interfacing units are allocated at their bounds: MW-to-optical (MW/O) and optical-to-MW (O/MW) converters. Between the interfaces, there are various photonics processing units for transmission, switching, distribution, filtration, time delaying, amplification, and frequency conversion of microwave signals in optical domain.

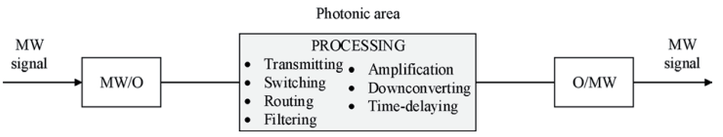

Figure 1.
A typical arrangement of MWP circuit.

3. Preselecting a feasible software to design MWP-based REAs

In the process of design, a developer of new MWP-based REA is facing a problem of choosing an appropriate software tool. As of today, the existing optical and optoelectronic CAD tools (OE-CAD) based on so-called Photonic Design Automation (PDA) platform are not developed like CAD tools intended for modeling of RF and MW circuits (MW-CAD) based on so-called Electronic Design Automation (EDA) platform that have been underway for about 5 decades. So today, to solve the problems of successful introducing MWP technique to the next-generation REAs, their individual units, and devices, there are various PDA-based CAD systems that allow creating complex models of varying difficulty. In general terms, all specialized CAD systems can be divided into a group for the structural design of optical linear and nonlinear media on various materials and a group for system modeling, in which individual devices are introduced as closed models with a set of specific characteristics.

Following it, currently, some commercial CAD systems have been developed for modeling optical and optoelectronic devices and systems based on PDA platform. The most popular representatives are VPI Photonics Design Suite from VPI Photonics, OptiSystem from Optiwave Design Software, and so on. However, our design experience in such OE-CAD systems clearly showed that they are most applicable for modeling complex apparatuses and systems, rather than individual device. In particular, the models of optical and optoelectronic components studied below are presented in the VPI-PDS tool in the form of ready-made library models with a very limited number of parameters necessary for their development. Therefore, based on this software, it is impossible to carry out detailed modeling of their functioning. For example, it is impossible to calculate a transfer characteristic in the large-signal mode taking into account introduced nonlinear distortions and also an influence of spurious elements of the input/output circuit and chip construction in the MW band.

To overcome this serious drawback, we almost 10 years ago proposed a different approach using a device-oriented MW-CAD tool [5], which was subsequently expanded in Ref. [13]. Its essence is that the optimal solution to the problem of modeling MWP components and MWP-based devices according to the criteria of accuracy and time-of-decision should be based on a rational combination of structural [in the form of an physical equivalent circuit (FEC)] and structureless models (when the response of the device is described in frequency, temporal, and spatial areas based on external input and output characteristics) of circuit elements. The effectiveness of this approach, called end-to-end multiscale design, has been confirmed experimentally, for example, when modeling optoelectronic devices with a MW passband [21]. Below, we briefly characterize both classes of CAD tools using the example of AWRDE and VPI-PDS.

3.1 Available microwave-electronic software characterization

The AWRDE is a comprehensive EDA platform for developing RF/microwave products that provide radio engineers with integrated high frequency, system, and electromagnetic (EM) simulation technologies and design automation to develop physically realizable electronics ready for manufacturing. The tool helps designers manage complex integrated circuit (IC), package, and printed-circuit board modeling, simulation, and verification, addressing all aspects of circuit behavior to achieve optimal performance and reliable results for first-pass success. The unique AWRDE tool features are the following:

- Unified design capture provides front-to-back physical design flow with dynamically linked electrical and layout design entry. Components placed in an electrical schematic automatically generate a synchronized physical layout based on libraries of standard, customized, and/or vendor-provided components.

- Design flow supports complex hierarchical projects with parameterized subcircuits for easy optimization and tuning. Circuit, system, or EM-based subcircuits can be quickly developed and used to populate larger, more complex networks common in today's RF front-end circuitry.

- Interoperability with industry-standard tools enables the exchange of design data for schematic or netlist import, bidirectional EM cosimulation, electrical or design rule check, and production-ready export. Additionally, powerful yield analysis and optimization address manufacturing tolerances for more robust designs and greater profitability.

- Customization due to the powerful application-programming interface extends the capabilities of the software using popular programming languages, providing user-defined scripts for automating common or complex tasks and custom design flows.

3.2 Available photonic software characterization

VPI-PDS sets the industry standard for end-to-end PDA comprising design, analysis, and optimization of components, systems, and networks that provide professional simulation software supporting requirements of active/passive integrated photonics and fiber optics applications, optical transmission system and network applications, and cost-optimized equipment configuration. The unique VPI-PDS tool features are the following:

- Link engineering solutions provide simple means for the cost-effective optical network configuration and offer a unified approach to control equipment libraries and engineering methodologies.

- Transmission design solutions provide professional means for investigating and optimizing system technologies and evaluating novel component and subsystem designs in a system context.

- Component design solutions provide professional means for the development and optimization of photonic ICs, optoelectronic components, and fiber-based amplifiers and lasers.

- Device simulation solution provides a versatile simulation framework for the analysis and optimization of integrated photonic waveguides and optical fibers.

3.3 Contention of the possibilities

In process of development of such MWP REAs combined microwave and photonic circuits, there was a problem to use an optimum computer product for their modeling and design. The essence is that for the accurate solution of an issue for modeling of such complicated systems containing radio engineering and optical

#	Feature	Realization	
		By MW-CAD (AWRDE)	**By OE-CAD (VPI-PDS)**
1	Analysis approach	Building blocks, 3D electromagnetic analysis	Building blocks
2	Simulation methods		
	• Linear circuits	S- and Y-matrices, equivalent circuits	S-matrices
	• Nonlinear circuits	Harmonic balance engine ALPAC, 3D planar electromagnetic simulator AXIEM modeling	S-matrices, combination of time-and-frequency domain modeling
3	Element representation		
	• Active microwave elements	Multirate harmonic balance, HSPICE, Volterra, based on measured characteristic models	Ideal or based on measured characteristic models
	• Active MWP elements	Absent	Rate equation-based, transmission line models
	• Passive elements	Lumped and distribution, microwave band specialties	Lumped, ideal
4	Possibility for calculating the key parameters of MWP circuits and links	By one-click operation	By user-created complicated schemes
5	IC layout design and analysis	Yes	No
6	Built-in design kits from the main foundries	Yes	No
7	Parameter optimization	Yes	No
8	Sensitivity analysis	Yes	No
9	Design of tolerance	Yes	No
10	Statistical design	Yes	No
11	Yield optimization routine	Yes	No
12	Built-in library of producer-specific models	Yes	No

Table 1.
Comparison of modern ME-CAD and OE-CAD tools.

elements and devices, the specialties of their functioning in both ranges must be taken into consideration. In this regard, more than 20 years ago, the conclusion was drawn that the optimal way for increasing the accuracy of MWP circuits taking into account the influence of their parasitic elements in MW band requires use of the high-power MW-CAD tool working at the symbolical level [19]. **Table 1** lists the detailed comparison of typical modern OE-CAD tool VPI Photonics Design Suite of VPI Photonics and well-known MW-CAD tool AWRDE of Cadence.

In result, the following outputs to optimally design the MWP-based REAs can be drawn out:

1. The available OE-CAD platform is most applicable for analyzing complex devices and systems, rather than their individual components, which are presented in the form of parameterized or formal library models with a very limited number of parameters necessary for accurate development of

MWP-based REAs. In particular, MW REA's passive elements such as waveguides, couplers, resonators, resistors, capacitor, and inductor represent only by ideal lumped models. In addition, calculating the key parameters of MWP circuits and links, such as large-signal transmission gain, noise figure, phase noise, intermodulation distortion, and intercept points is possible only by user-created complicated testbeds. While on MW-CAD platform, they are calculated using a 'one-click' operation.

2. From the developer's point of view, the OE-CAD platform lacks (or is just starting to appear) a large number of functions that are very useful for investigating the device under design (see items 5–12 of **Table 1**).

3. The main disadvantage of the MW-CAD platform is the lack of models of active optoelectronic components such as semiconductor lasers, photodiodes, and electro-optic modulators.

4. Our multiyear experience in CAD of MWP devices using AWRDE tool has shown that the most convenient way to introduce optoelectronic devices is to present them as a behavioral model in the form of a nonlinear physical equivalent circuit. In this circuit, the linear section is built on the basis of passive lumped or distributed components, and the nonlinear one uses sources (current, voltage, noise, etc.), the characteristics of which are based on experimental data.

4. Comparative computer-aided design

Having clarified the principal pros and cons of the two classes of software tools from the point of view of designing MWP-based REAs, in this section, we exemplify specifically the results of their comparative calculation for various devices and systems.

4.1 Calibration of optoelectronics and optical element models

To conduct accurately comparative modeling of MWP REAs, it is necessary to perform a reciprocal calibration for the models of optoelectronic and optical components. In this regard, the behavioral models in the AWRDE are initially more accurate, since they are based on experimental data. That is, the calibration consists in fitting the parameters of the VPI-PDS models so as to obtain close basic characteristics in small- and large-signal modes. Below, we present and discuss the results of model calibration for key optoelectronic and optical components, based on which a set of subsequent simulations for basic REAs will be carried out in the next subsection.

4.1.1 Semiconductor laser source

Variants of AWRDE-based semiconductor laser source (SLS) model in the form of FECs are proposed and described in detail in Refs. [5, 6, 13, 18]. On the other hand, there are more than 10 library models of SLS in VPI-PDS tool mainly based on linear or nonlinear rate equations differing in the way they are presented and in the set of input data. **Figure 2** exemplifies the result of small-signal frequency response (mod. S_{21}) simulations using AWRDE's single-carrier model [18] and VPI-PDS's "LaserRateEqSM.vtms" model. As follows from the figure, both graphs

for this reciprocally calibrated optoelectronic element have a similar appearance with typical conversion losses of about 30 dB, about 3-dB rise associated with the so-called electron-photon resonance, and −3-dB direct modulation bandwidth of slightly larger than 11 GHz.

4.1.2 Electro-optical modulator

The AWRDE-based electro-optical intensity modulator (EOM) model of so-called electroabsorption type in the form of FECs is proposed and described in detail in Ref. [13]. On the other hand, there are two library models of electroabsorption modulator (EAM) in VPI-PDS tool differing in the way they are presented and in the set of input data. **Figure 3** exemplifies the result of large-signal optical spectra simulations using AWRDE model [13] and VPI-PDS's "ModulatorEA_Polynomial.vtms" model. As follows from the figure, both graphs for this reciprocally calibrated optoelectronic element have a similar appearance with approximately the same power levels of the fundamental signal and the first two harmonic distortions caused by the nonlinearity of the modulator's transfer characteristic.

4.1.3 PIN-photodiode

Variants of AWRDE-based pin-photodiode (PD) model in the form of FECs are proposed and described in detail in Refs. [7, 8, 13, 18]. On the other hand, there are only one unified model of PD in VPI-PDS tool that is ideal and handles both single-mode and multimode optical signals. **Figure 4** exemplifies the result of small-signal frequency response simulations using AWRDE model [13] and VPI-PDS's "Photodiode.vtms" model. As follows from the figure, both graphs for this reciprocally calibrated optoelectronic element have a similar appearance. However,

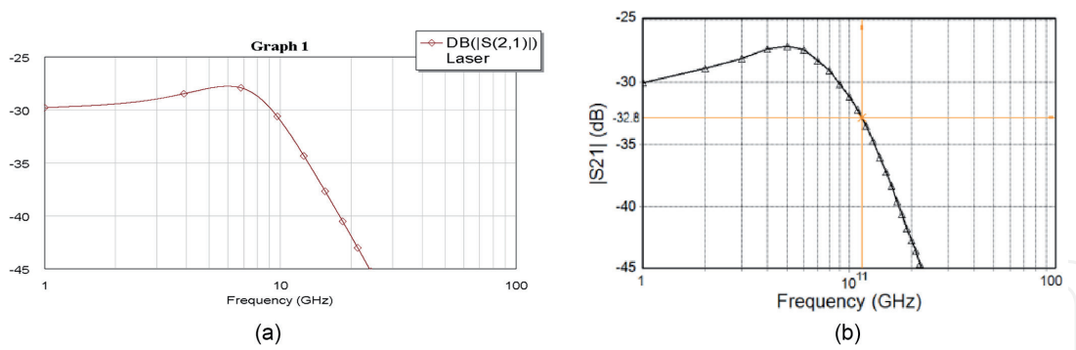

Figure 2.
Small-signal frequency response of the semiconductor laser source model by (a) AWRDE and (b) VPI-PDS.

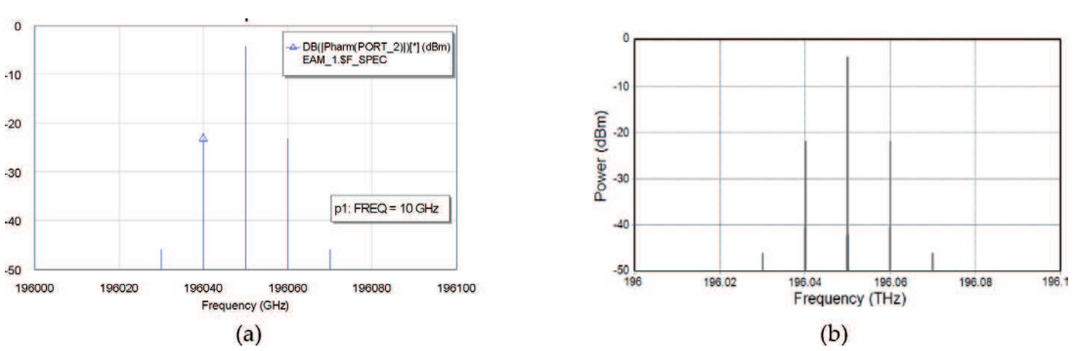

Figure 3.
Large-signal optical spectrum of the electro-optical modulator model by (a) AWRDE and (b) VPI-PDS.

using the same reference data, a −3-dB bandwidth was obtained a little more than 20 GHz for the AWRDE model and 27 GHz for the VPI-PDS model.

The most probable reason for this meaningful discrepancy is explained by the ideality of the VPI-PDS model, which does not take into account the influence in MW band of either the photodiode chip itself or the parasitic elements of its output circuit. Specifically, in order to obtain a reasonable decrease in the frequency response at higher frequencies, a library model of a low-pass filter had to be introduced at the PD model output. Effect referred to parasitic circuit elements may be clearly explained by **Figure 5**. It follows from the AWRDE graphs that a designer can realized twofold expansion of the PD's 3-dB passband (20–40 GHz) owing to the appropriate fitting of the connecting wire inductance L_w.

4.1.4 Optical fiber

In general, with the wave approach, where light is regarded as an EM wave, any optical passive element, including the optical fiber (OF), can be simulated in the same way in MW-CAD or in OE-CAD tool. Namely, in AWRDE, a segment of optical fiber of a certain length can be equivalently represented using, for example, the library model of physical transmission line with loss (TLINP). However, when constructing a realistic model of an OF, a whole set of additional effects should be taken into account, such as dispersion, reflection, scattering, nonlinearity, and ambient temperature, the influence of which can degrade the transmission characteristic. The AWRDE-based OF model in the form of FECs taking into account the above limiting factors is proposed and described in detail in Ref. [15]. On the other hand, there are as many as nine library models of multimode or single-mode OF in VPI-PDS tool differing in the way they are presented, which deteriorating factors and what set of input data are taken into account. **Figure 6** exemplifies the result of

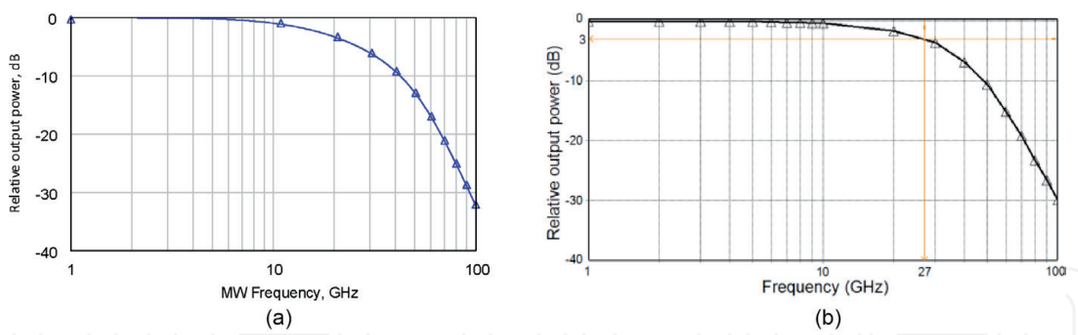

Figure 4.
Small-signal relative frequency response of the PIN-photodiode model by (a) AWRDE and (b) VPI-PDS.

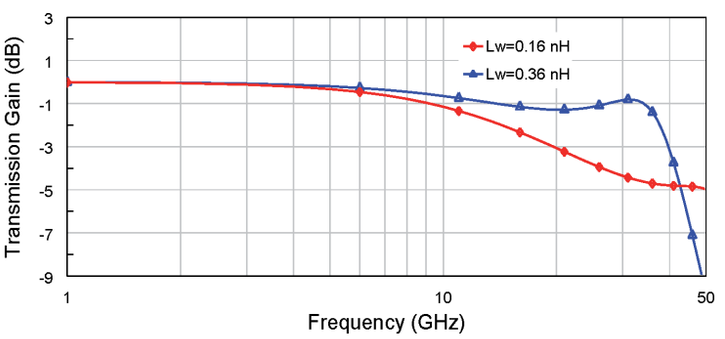

Figure 5.
Effect of the connecting wire between photodiode chip and output pad.

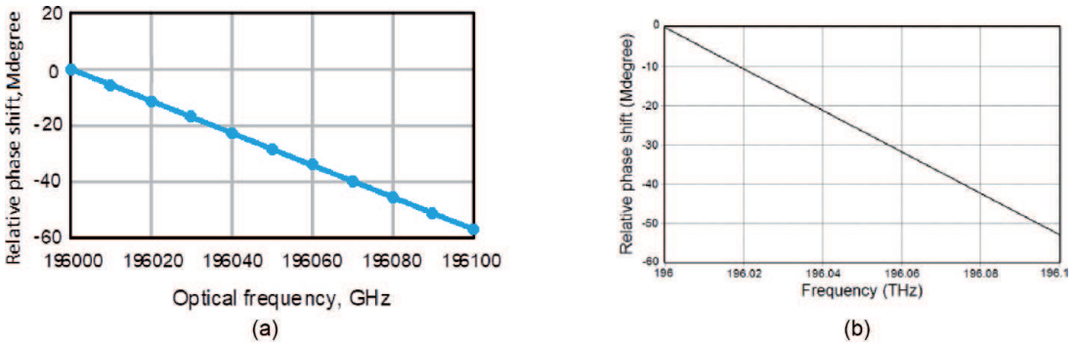

Figure 6.
Relative phase-frequency response of the single-mode optical fiber model by (a) AWRDE and (b) VPI-PDS.

small-signal phase response (arg. S_{21}) simulations using AWRDE's simplified model [18] and VPI-PDS's "UniversalFiberFwd.vtmg" model. As follows from the figure, both graphs for this reciprocally calibrated optical element have a similar appearance and the same slope.

4.1.5 Reference data for the further simulation experiments

The purpose of this subsection is to generalize the results of the reciprocal calibration for optical and optoelectronic component models in such a way as to provide unified reference data on their parameters for further studies. **Table 2** lists the common reference data for four above-considered models of SLS, EOM, PD, and OF as well as of electronic amplifier typically used after pin-PD.

4.2 Simulation examples

In this subsection, the subjects of the study are the specific microwave photonics (MWP) devices and apparatuses such as a delay circuit, oscillator, frequency converter, and fiber-wireless fronthaul of 5G mobile communication system. The tools for the comparative computer simulation are well-known commercial software AWRDE and VPI-PDS. The research takes into account some key distortion sources of the MW signal under processing such as introduced noise and nonlinear distortion of active optoelectronic elements as well as chromatic dispersion of the optical fiber. The parameters for the elements to be used are based on the data of **Table 2**.

4.2.1 MW-signal's optical delay circuit

Fiber-optic delay circuit is one of the most feasible MWP units [22]. **Figure 7** shows the block diagram of the single-channel optical delay circuit (ODC) under test including semiconductor laser that directly modulated by input MW signal, optical fiber, the length of which corresponds to the required delay time, and a photodetector, at the output of which a delayed MW signal is formed. Following it, below we will describe two models and some comparative simulation results using AWRDE and VPI-PDS tools.

4.2.1.1 Modeling in VPI-PDS

Figure 8 demonstrates the model for the simulation experiment evaluating some key quality parameters for ODC under test when transmitting continuous wave MW signals. As one can see, it contains the same ODC layout as in **Figure 7**

Parameter		Value
Semiconductor laser source	Operating current	40 mA
	Average power	8 mW
	Optical carrier	C-band (191 to 196.1 THz)
	Linewidth	1.5 MHz
	Relative intensity noise	−150 dB/Hz
	Threshold current	8.5 mA
	Slope efficiency	0.14 W/A
	Direct modulation 3-dB bandwidth	Up to 11 GHz
Electro-optical modulator (EAM)	Operating voltage	−0.6 V
	Extinction ratio	14 dB
	Slope efficiency	0.14 W/V
	Linewidth enhancement factor (α)	1.0
	3-dB modulation bandwidth	30 GHz
PIN-photodiode	Responsivity	0.7 A/W
	Dark current	100 nA
	Optical input power	<3 mW
	3-dB passband	Up to 30 GHz
Post-amplifier (if needed)	Gain	40 dB
	Noise spectral density	20×10^{-12} A/Hz$^{1/2}$
Optical fiber	Type	SMF-28e+
	Length	Up to 20 km
	Attenuation	0.2 dB/km
	Dispersion	17 e^{-6} s/m^2
	Dispersion slope	80 s/m^3

Table 2.
Reference data of elements for the further study.

consisting of the calibrated in the previous subsection library model for single-mode laser, so-called galactic model for optical fiber also including delay element, and library models for pin-photodiode and electrical post-amplifier.

4.2.1.2 Modeling in AWRDE

The layout of single-channel ODC [15] is very simple and contains (**Figure 9**) the subcircuit models of SLS, single-mode optical fiber of a corresponding length (delay ≈4.8 ns/m), and PD.

4.2.1.3 Simulation results

Figure 10 exemplifies the simulation results for ODC's group time delay (GTD), where the MW signal frequency is swapped in the range of 1–7 GHz, and the OF length is 3 m. As follows from the figure, due to the broadband of the constituent elements, the delay does not change in such a wide frequency range of modulating frequencies (almost 3 octaves). Its value coincides with high accuracy for both

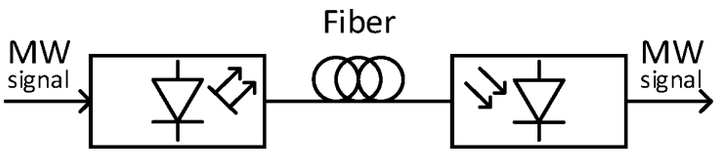

Figure 7.
Block diagram of the optical delay circuit under test.

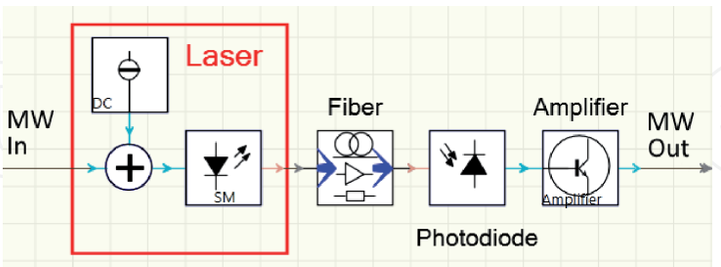

Figure 8.
VPI-PDS's model of fiber-optic delay circuit of MW signals.

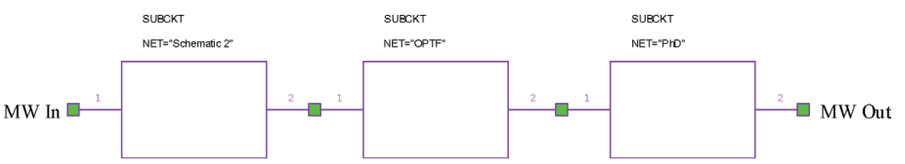

Figure 9.
AWRDE model of fiber-optic delay circuit of MW signals.

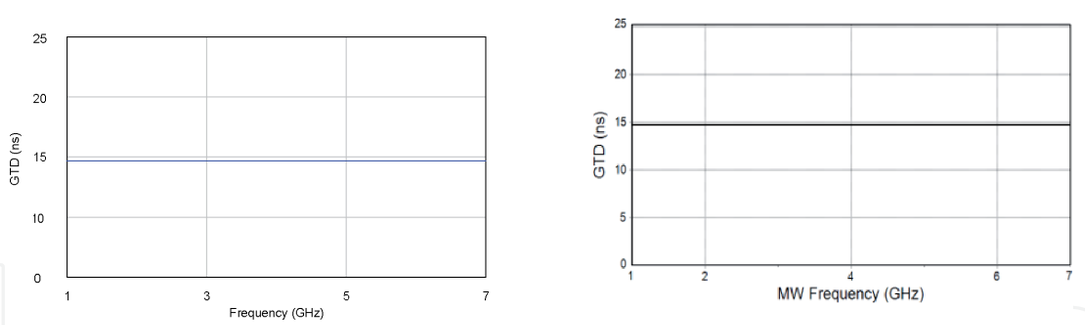

Figure 10.
Examples of the simulation results for FODC of MW signals: relative phase-frequency response by (a) AWRDE and (b) VPI-PDS.

models and is close to the above delay in a standard single-mode fiber. In addition, **Figure 11** demonstrates the large-signal amplitude characteristic of the ODC under test. As one can see from the figure, 1 dB input compression point is near −10 dBm for the both models.

The following outputs can be drawn from our study:

- The investigated optoelectronic delay circuit is a very simple device that, in contrast to the electronic analog, provides an extremely wide operating bandwidth and, thanks to the very short delay time in electro-optical and optical-electric converters and low losses in an optical fiber, an extremely wide delay range from units of nanoseconds to hundreds of microseconds.

- Both computer tools under study provide approximately the same accuracy of calculations, which coincide with the actual value of the delay in the fiber [22]; however, the AWRDE model is simpler and more flexible.

4.2.2 Optoelectronic oscillator of MW signals

Figure 12 presents the block diagram of the MW signal's optoelectronic oscillator (MW-OEO) that is another worldwide example of MWP application [23]. Generally, it contains two requisite sections: optical one and electrical one. Here, the optical section includes SLS, EOM, OF, and PD. The electrical section includes low-noise MW amplifier (LNA), band-pass filter (BPF), power MW amplifier (PA), and electrical coupler (EC).

4.2.2.1 Modeling in VPI-PDS

Following a similar approach as in our previous computation modeling, **Figure 13** shows a VPI-PDS model of MW-OEO [10]. An important specificity of this model is in taking a phase noise of SLS into consideration.

Note that due to the absence in this software the library model of optical fiber (OF) that takes into account the delay in it, the OF model in the diagram has been replaced by library models of the optical attenuator and the delay element with identical parameters.

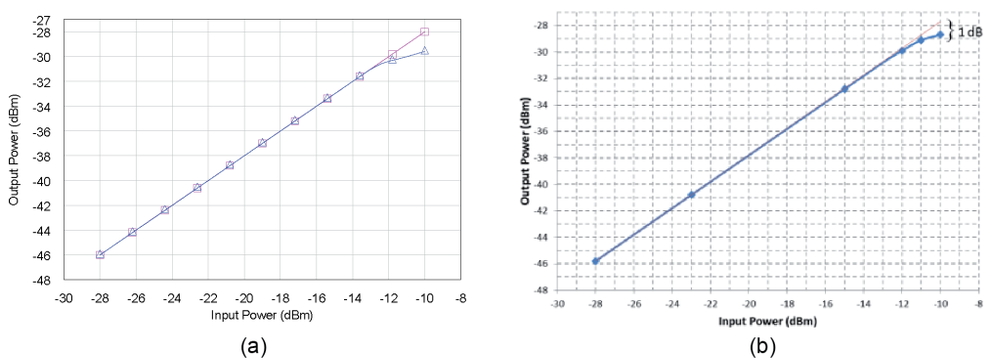

Figure 11.
Simulated large-signal power characteristic for the FODC of MW signals under test by (a) AWRDE and (b) VPI-PDS.

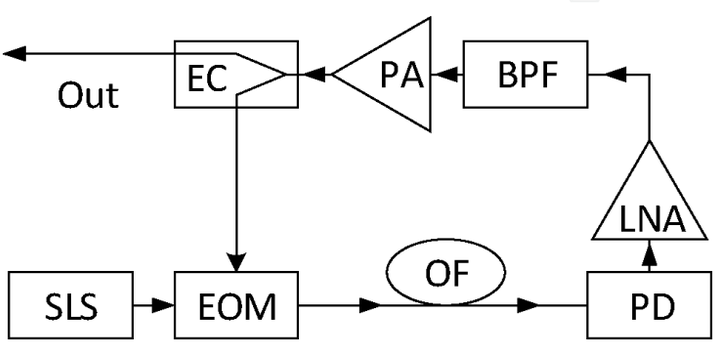

Figure 12.
Block diagram of the MW-OEO under test.

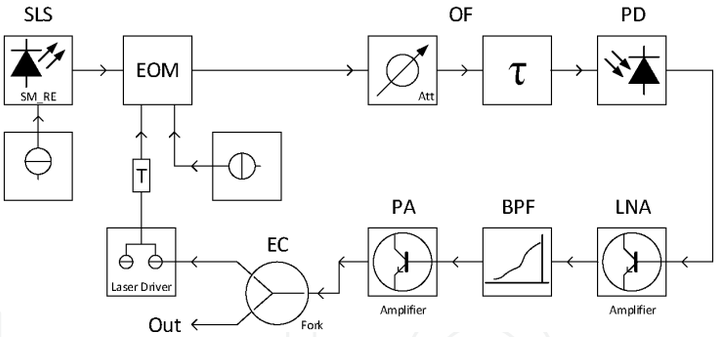

Figure 13.
VPI-PDS's model of optoelectronic oscillator of MW signals.

4.2.2.2 Modeling in AWRDE

Figure 14 represents circuit-level nonlinear model of the MW-OEO under study realized by AWRDE software. The diagram includes a chain of subcircuits (SUBCKTs) representing (from left to right): small-signal (including noise) and large-signal features of SLS (see Section 4.1.1), delay and losses of OF, nonlinear optical-to-electrical conversion feature of PD (see Section 4.1.3), gain and bandwidth of LNA, bandwidth and losses of BPF, frequency and amplitude features of PA, and couple of EC models realized by AWRDE tool. Besides, there are two service program elements mitigating self-sustained oscillation in the return path of the model: ideal DGDELAY that models an ideal, linear, frequency-dependent, digital time delay element and OSCAPROBE that initiates a large-signal oscillator simulation.

4.2.2.3 Simulation results

As an example, **Figure 15** presents phase noise characteristics for MW-OEO of 9 GHz simulated by the OE-CAD tool (black line) and by the MW-CAD tool (red curve). As one can see, there is a significant discrepancy in the simulation results at the offsets more than 100 kHz.

The following outputs can be drawn from our study:

- With small offsets from the MW carrier, the phase noise levels calculated using both software approximately coincide with each other and with experimental data [9].

- With large offsets, the discrepancy between the AWRDE-calculated and experimental data does not exceed 2 dB [9], which indicates the more validity of its model.

- To measure the phase noise of an oscillator, there is a built-in model of the noise analyzer (OSCNOISE) in the AWRDE tool, while to perform this operation in the VPI-PDS tool, it is necessary to create a complex testbed.

4.2.3 Optoelectronic frequency converter of MW signals

About 10 years ago, we proposed a simple circuit for an optoelectronic frequency converter (OEFC) of MW signals, in which the nonlinearity of a SLS's

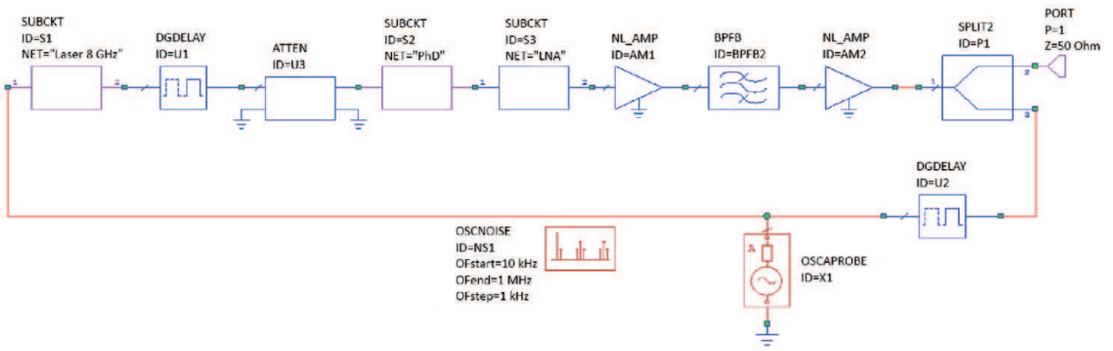

Figure 14.
AWRDE's model of optoelectronic oscillator of MW signals.

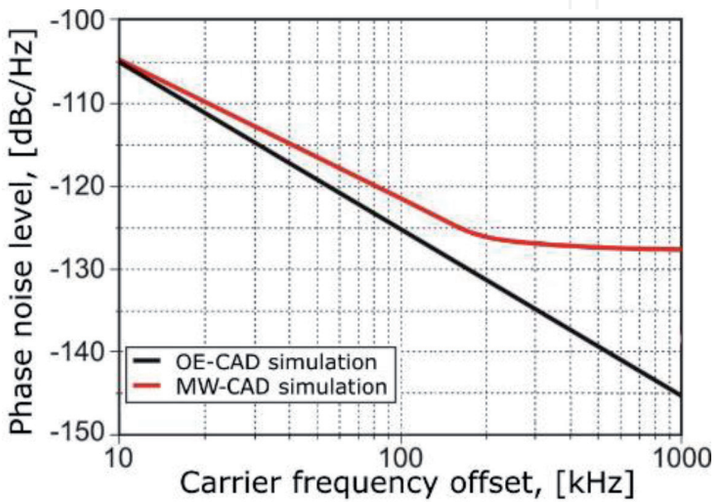

Figure 15.
Phase noise characteristics (RIN = −150 dBc/Hz).

light-current characteristic is leveraged [11]. The efficiency of this device was confirmed by modeling in VPI-PDS and experimental research at input frequencies of 1 and 1.5 GHz. Later, the operation of this device was modeled in AWRDE tool at other frequencies of the MW input signals [10]. The block diagram of the OEFC containing an electronic power combiner mixing the RF and LO MW-signals, a SLS, a pin-PD, and an electronic bandpass filter to isolate the mixing product is shown in **Figure 16**.

4.2.3.1 Modeling in VPI-PDS

Following a similar approach as in our previous computation modeling, **Figure 17** depicts a VPI-PDS model of MW-OEFC [11]. Its appearance repeats the diagram of **Figure 16** with the introduction of an electronic attenuator (El), which serves to adjust the level of MW signals at the input of the SLS.

4.2.3.2 Modeling in AWRDE

Following the above block diagram, **Figure 18** demonstrates the OEFC model under investigation in AWRDE environment. This figure includes a chain of subcircuits representing (from left to right) SLS (first three sections) and pin-PD (right sections) nonlinear models realized by AWRDE tool (see Sections 4.1.1 and 4.1.3). The laser model is presented by the FEC of the linear sections of the SLS model (S2) together with the test fixture model (S1) and nonlinear section (A1) representing

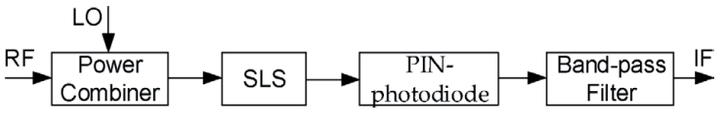

Figure 16.
Block diagram of the MW-OEFC under test.

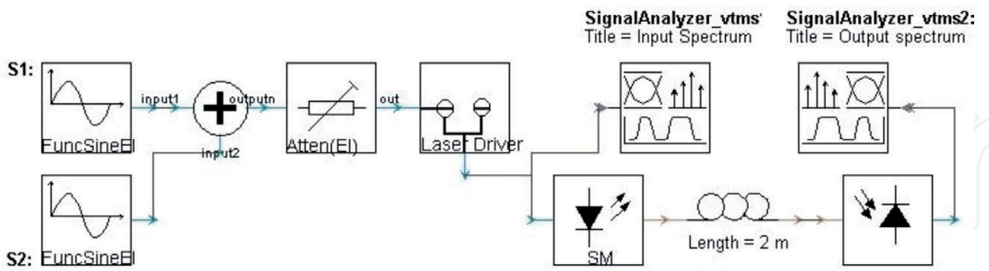

Figure 17.
VPI-PDS's model of optoelectronic frequency converter of MW signals.

AWRDE's library element LOOKUP that implements a lookup table including its measured light-current characteristic. The right section of the chain is nonlinear PD FEC model. Simulation details are reported in Ref. [10].

4.2.3.3 Simulation results

Figure 19 shows the results of simulation experiment referred to defining output spectra of the OEFC under investment by AWDE MW-CAD tool (a) and VPI-PDS OE-CAD tool (b). In both procedures, the input RF signal had a power of −20 dBm at a frequency of 1 GHz, and LO signal had a power of 6 dBm at a frequency of 1.5 GHz.

The following outputs can be drawn from our study:

- As one can see from **Figure 19(a)**, applying powerful harmonic balance method of AWRDE software resulted in output (IF) signal power near −55 dBm at a frequency of 2.5 GHz, that is, conversion gain is −35 dB. The rest of the peaks in the figure represent clearly the full output spectrum of standard microwave mixer in agreement with well-known formula $|mF_{RF} \pm nF_{LO}|$, where m and n are integers. On the other hand, **Figure 19(b)** shows a comparable result referred to conversion gain, however, a significant part of the mixing products either differs in level or is absent altogether.

- The results of simulation using the proposed AWRDE models should be closely matched to the experimental ones because their parameters are constructed on the measured characteristics of laser and photodiode.

4.2.4 Fiber-wireless fronthaul of 5G mobile communication system

In the framework of 5G's Radio-over-Fiber (RoF) concept, fiber-wireless fronthaul network (FWFN) is one of the promising ways to deliver intensive digital traffic with seamless convergence between wired optical backhaul and fiber-wireless fronthaul, which is important to keep the remote cells flexible, cost effective, and power efficient [4, 17]. The block diagram of the FWFN containing Central station (CS) and a set of Remote stations (RS) interactively connected to CS via fiber-optics links (FOL) is shown in **Figure 20**. A typical position of RS is in the

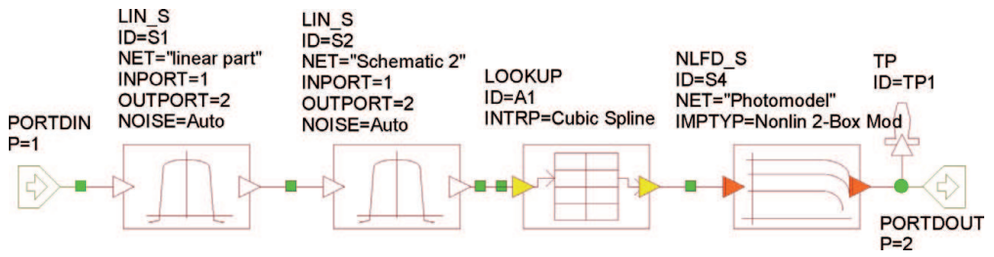

Figure 18.
Circuit-level AWRDE's optoelectronic MW-frequency converter model.

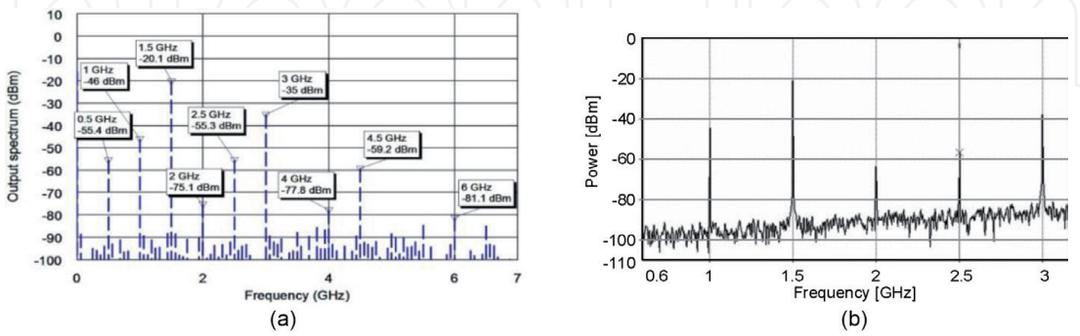

Figure 19.
Large-signal optoelectronic MW frequency converter output spectra by (a) AWRDE and (b) VPI-PDS.

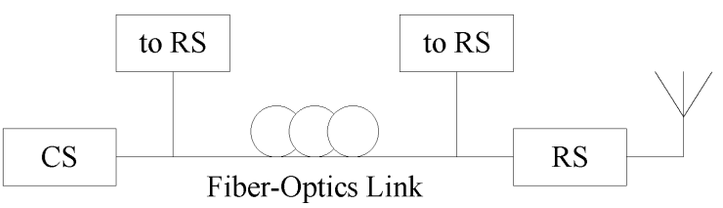

Figure 20.
Block diagram of the fiber-wireless fronthaul network under test.

center of the service area; that is, for omnidirectional covering, four phased array antennas with an azimuth of 90° would be an optimal decision [14, 16].

4.2.4.1 Modeling in VPI-PDS

Figure 21 depicts the VPI-PDS's model of downlink channel for FWFN under study that has the same block diagram as in **Figure 20**.

As one can see from the figure, there are three parts such as CS, FOL, and RS. The first one includes the set of library models imitating quadrature amplitude modulated (QAM) MW transmitter as well as the models of SLS and EOM calibrated in Section 4.1. The second one consists of the library model of polarization controller and the model of OF calibrated in Section 4.1. Finally, the third one includes the model of pin-PD calibrated in Section 4.1 as well as the set of library models imitating QAM MW receiver. A detailed description of the QAM transmitter and receiver models is given in Ref. [15].

4.2.4.2 Modeling in AWRDE

Figure 22 depicts AWRDE's model of downlink channel for FWFN under study. The model has the same arrangement as in **Figure 21** excluding the transmitting part

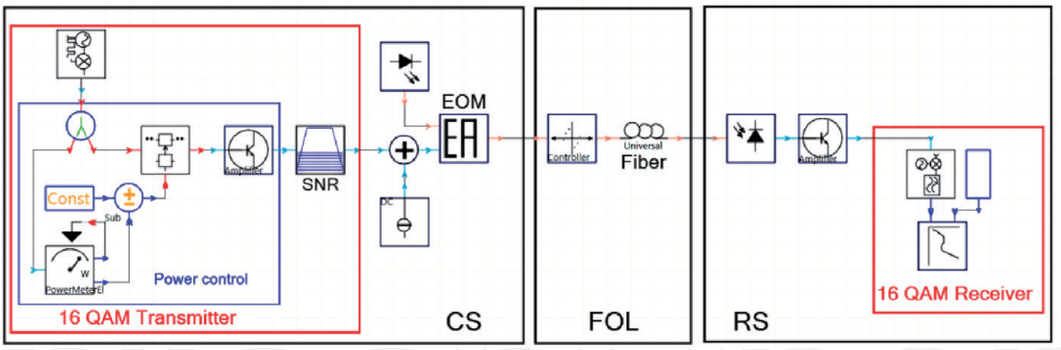

Figure 21.
VPI-PDS model of downlink channel for a fiber-wireless fronthaul network.

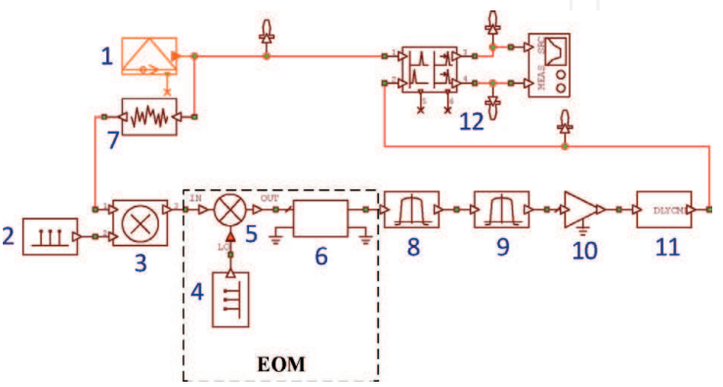

Figure 22.
AWRDE model of fiber-wireless fronthaul network. 1, QAM generator; 2, MW tone generator; 3, multiplexer; 4, quasi-optical signal generator; 5, behavioral mixer; 6, optical frequencies splitter; 7, MW noise generator; 8, model of single-mode fiber as subcircuit; 9, model of photodiode as subcircuit; 10, post-amplifier; 11, signal delay compensator; 12, vector signal analyzer.

that contains the library model of quasi-optical tone generator imitating laser carrier, the library model of multiplexer that performs the operation of upconverting signal to the optical range, and a passive subcircuit representing frequency response of the EOM under test in S2P format. Note that earlier we proposed and described in detail [13] a nonstructural nonlinear model for the EOM of the EAM type suitable for developers of local telecommunication systems based on RoF technology. However, here, its simplified model with the parameters calibrated in Section 4.1 is used.

4.2.4.3 Simulation experiment

In this section, the subject of the study is a MWP-based FWFN; the devices of study are SLS, EOM, single-mode OF, and PD, which parameters have been calibrated in Section 4.1. The tools for the computer simulation are two well-known commercial program environments such as OE-CAD VPI-PDS and MW-CAD AWRDE. The study took into account the key distortion sources of the transmitted signal: noises of the laser, chirp of the modulator, and losses and chromatic dispersion of the fiber. To eliminate the influence of nonlinear effects during modulation and signal transmission through the fiber, MW and optical signal levels were selected, so that the modulation index did not exceed 30%, and the optical power in the fiber was below 5 mW.

4.2.4.4 Reference data

Table 3 lists the common reference data for the simulation experiment.

Parameter	Value
Length of pseudo-random bit sequence	2^{15}–1
Bitrate	2.5 Gbit/s
RF carrier frequency	25 GHz
Input RF power	–11 to –26 dBm
Type of RF modulation	16-QAM
Type of optical modulation	Intensity

Table 3.
Common reference data for the FWFN under study.

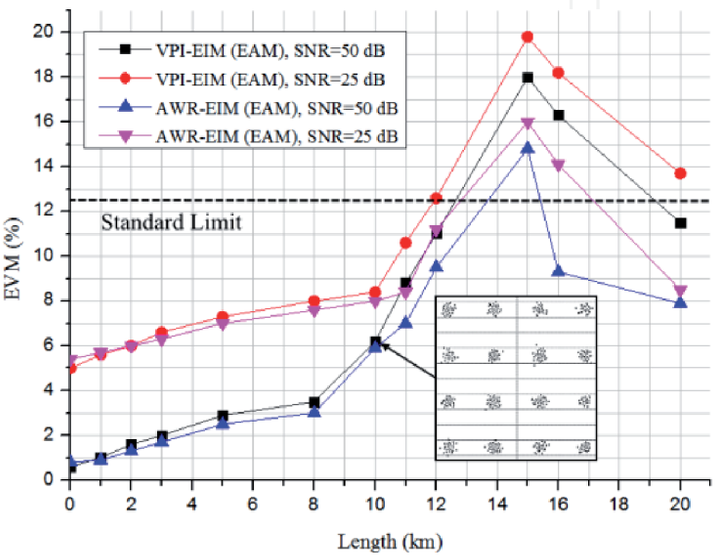

Figure 23.
EVM versus fiber length characteristics.

4.2.5 Simulation results

In preparation for the simulation experiments, the modulation index of each device under study was optimized in such a way as to ensure the maximum output MW carrier-to-noise ratio while maintaining the low-signal mode at the modulating frequency. **Figure 23** depicts an example of comparative simulation of Error Vector Magnitude (EVM) versus fiber length characteristics for the FWFN under study during transmission of 2.5 Gbit/s and 16-QAM MW signal at the frequency of 25 GHz using signal-to-noise ratio (SNR) of 50 and 25 dB. For the best vision, there is the inset in the figure showing constellation diagrams at the fiber length of 10 km. In addition, the dotted line indicates the standard limit of the EVM during transmission of the 16-QAM signal, which is 12.5%.

The following outputs can be drawn from our study:

- the EVM versus fiber length characteristics simulated by both the software closely coincide with each other at the signal-to-noise ratio of 50 and 25 dB within the FOL distance of up to 10 km and

- for longer FOL lengths, all characteristics show a peak that exceeds the standard limit, caused by the effect of chromatic dispersion [22].

5. Conclusion

The chapter is devoted to recovering the optimal principle to computer-aided design a new class of microwave band radio electronic apparatuses using microwave-photonics approach to effectively generate, transmit/receive, and process super wideband radio signals in near infrared optical range meeting minimum insertion loss of a quartz light guide. Preselecting a feasible software instrument to design MWP-based radio engineering apparatuses showed that up to date, exploiting for some decades microwave band software tools based on electronic design automation platform are preferable than relatively rudimentary software tools based on photonic design automation platform due to much more possibilities to produce the state-of-art radio engineering devices, apparatuses, and systems. In addition, the problem referred to the reasonableness and accuracy of calculations comes to the fore because in the second tool all active and passive electronic and photonic circuit elements are presented as ideal models with lumped parameters that do not take into account frequency distortion due to spurious elements and transmission lines with distributed parameters. To clear the fact and estimate the impact, a comparative modeling for four basic radio electronic apparatus designed on the microwave-photonics approach, such as optical delay circuit, optoelectronic oscillator, optoelectronic frequency converter, and 5G's fiber-wireless fronthaul link, was carried out using two widespread off-the-shelf software: VPI Photonics Design Suite (VPI-PDS) and Applied Wave Research Design Environment (AWRDE). The following outputs can be derived, which a developer should take into consideration. The advantage of the simulation in VPI-PDS software is its greater convenience and speed with acceptable calculation accuracy since the built-in library models of optoelectronic and optical components are mainly used. On the other hand, the gain of the simulation in AWRDE software is a more sophisticated and, at the same time, a more accurate characterization because their parameters are constructed on the measured characteristics of active optoelectronic components, so the results should be closely matched to the experimental ones. Our future work will focus on the upgrading already proposed models and designing new AWRDE models of devices and units for microwave photonics applications.

Acknowledgements

This work was supported by the Russian Foundation for Basic Research, Grant Nos. 17-57-10002 and 18-29-20083.

Conflict of interest

The authors declare the lack of the 'conflict of interest'.

Author details

Mikhail E. Belkin[1*], Tatiana Bakhvalova[1], Vladislav Golovin[2], Yuriy Tyschuk[2] and Alexander S. Sigov[1]

1 Scientific and Technological Center, "Integrated Microwave Photonics", MIREA—Russian Technological University, Moscow, Russian Federation

2 Sevastopol State University (SevSU), Sevastopol, Russian Federation

*Address all correspondence to: belkin@mirea.ru

References

[1] Gilbert KD, McClees HC, Lindsay PA, Paik SF. Photo-mixing experiments at X band. Proceedings of the IEEE. 1963;**51**(8):1148-1148. DOI: 10.1109/PROC.1963.2461

[2] Seeds AJ, Williams KJ. Microwave photonics. IEEE/OSA Journal of Lightwave Technology. 2006;**24**(12):4628-4641. DOI: 10.1109/JLT.2006.885787

[3] Capmany J, Novak D. Microwave photonics combines two worlds. Nature Photonics. 2007;**1**(1):319-330. DOI: 10.1038/nphoton.2007.89

[4] Waterhouse R, Novak D. Realizing 5G: Microwave photonics for 5G mobile wireless systems. IEEE Microwave Magazine. 2015;**16**(8):84-92. DOI: 10.1109/MMM.2015.2441593

[5] Belkin ME, Belkin L, Sigov AS, Iakovlev V, Suruceanu G, Kapon E. Performances of microwave-band analog signal transmission using wafer-fused long wavelength VCSELs. IEEE Photonics Technology Letters. 2011;**23**(20):1463-1465. DOI: 10.1109/LPT.2011.2162230

[6] Belkin ME, Iakovlev V. Microwave-band circuit-level semiconductor laser modeling. In: Proceedings of the 9th European Modeling Symposium on Mathematical Modeling and Computer Simulation EMS 2015, Madrid, Spain; 6-8 October 2015. pp. 1-3

[7] Belkin ME. Multiscale computer aided design of microwave-band P-I-N photodetectors. In: Gateva S, editor. Photodetectors. Croatia: InTech; 2012. pp. 231-250

[8] Belkin ME, Sigov AS. Circuit-level large-signal modeling of microwave bandwidth photodetector. In: Proceedings of the International Conference on Electromagnetics in Advanced Applications (ICEAA 2015); 7-11 September 2015; Torino, Italy. pp. 1587-1589

[9] Belkin ME, Golovin V. Microwave electronic CAD modeling of microwave-band optoelectronic oscillator based on long wavelength VCSEL. In: Proceedings of the International Conference on Microwaves, Communications, Antennas and Electronic Systems (COMCAS 2015), Tel Aviv, Israel; 2-4 November 2015. pp. 1-3

[10] Belkin ME, Tyschuk Y. Microwave electronic CAD modeling of microwave photonic devices based on LW-VCSEL mixing. In: Proceedings of the II International Conference on Microwave and Photonics (ICMAP 2015), Dhanbad, Bihar, India; 11-13 December 2015. pp. 1-3

[11] Belkin ME, Belkin LM, Loparev AV, Iakovlev V, Kapon E, Suruceanu G. Microwave-band optoelectronic frequency converters based on long wavelength VCSELs. In: Proceedings of the International Conference on Microwaves, Communications, Antennas and Electronic Systems (COMCAS), Tel Aviv; November 2011. pp. 1-6

[12] Belkin ME, Iakovlev V, Sigov AS, Tyschuk Y, Golovin V. An advanced approach to simulation of super-wide bandwidth information and communication systems combining microwave and photonic industrial technologies. In: Proceedings of the European Modelling & Simulation Symposium (EMSS2016), Cyprus; 26-28 September 2016. pp. 141-147

[13] Belkin ME, Golovin V, Tyschuk Y, Vasil'ev M, Sigov AS. Computer-aided design of microwave-photonics-based rf circuits and systems. In: Chapter 4 in Book IntechOpen RF Systems, Circuits and Components. 2018. pp. 61-81

[14] Belkin ME, Fofanov D, Golovin V, Tyschuk Y, Sigov AS. Design and optimization of photonics-based beamforming networks for ultra-wide mm Wave-band antenna arrays. In: Chapter 4 in Book IntechOpen Array Pattern Optimization. 2018. pp. 47-67

[15] Belkin ME, Bakhvalova T, Golovin V, Tyschuk Y, Sigov AS. Selecting an optimal computer software for design of microwave-bandwidth optoelectronic devices of a fiber-optics link. In: Proceedings of the European Modeling and Simulation Symposium (EMSS), Lisbon, Portugal; 18-20 September 2019. pp. 304-310

[16] Belkin ME, Fofanov D, Bakhvalova T, Sigov AS. Design of reconfigurable multiple-beam array feed network based on millimeter-photonics beamformers. In: Chapter in Book Array Pattern Optimization. Rijeka: IntechOpen; 2019

[17] Belkin ME, Bakhvalova T, Sigov AC. Design principles of 5G NR RoF-based fiber-wireless access network. In: Chapter to IntechOpen Book "Recent Trends in Communication Networks". 2019

[18] Belkin ME, Golovin V, Tyschuk Y, Sigov AS. A simulation technique for designing next-generation information and communication systems based on off-the-shelf microwave electronics computer tool. International Journal of Simulation and Process Modelling. 2018;**13**(3):238-254. DOI: 10.1504/IJSPM.2018.093104

[19] VPI Photonics Design Suite [Internet]. Available from: https://www.vpiphotonics.com/ [Accessed: 16 January 2020]

[20] Applied Wave Research Design Environment [Internet]. Available from: https://awrcorp.com/ [Accessed: 16 January 2020]

[21] Leijtens XJM, Le Lourec P, Smit MK. S-matrix oriented CAD-tool for simulating complex integrated optical circuits. IEEE Journal of Selected Topics in Quantum Electronics. 1996;**2**(2):257-262. DOI: 10.1109/2944.577373

[22] Urick VJ, McKinney JD, Williams KJ. Fundamentals of Microwave Photonics. New Jersey: Hoboken; 2015. DOI: 10.1002/9781119029816

[23] Yao XS. Opto-electronic oscillators. In: Chang WSC, editor. RF Photonic Technology in Optical Fiber Links. United Kingdom: Cambridge University Press; 2002. pp. 255-292. DOI: 10.1017/CBO9780511755729